

The relationship between the North Atlantic Oscillation and El Niño–Southern Oscillation

Jianping Huang, Kaz Higuchi and Amir Shabbar

Atmospheric Environment Service, Environment Canada, Downsview, Ontario, Canada

Abstract. We have applied a multiresolution cross-spectral analysis technique to resolve the temporal relationship between the NAO and ENSO. The study shows significant coherence between NAO and Niño3 SST in about 70% of the warm ENSO events from 1900 to 1995, of which 33% and 37% are associated with a 5- to 6-year period (E1) and a 2- to 4-year period (E2) oscillation terms in the spectral decomposition, respectively. The dominant teleconnection pattern associated with changes in the mean atmospheric circulation during the initial winter of a typical E1 and E2 events is the positive phase of the Pacific/North American (PNA) pattern. Non-coherence between the NAO and ENSO occurs during relatively weak Niño3 SST anomaly, with a teleconnection pattern which shows a strong negative phase of the NAO and a pattern which resembles a weak eastward shifted negative phase of the PNA pattern.

1. Introduction

Two of the major sources of interannual variability in the atmospheric circulation are the North Atlantic Oscillation (NAO) and the El Niño-Southern Oscillation (ENSO). Interannual variations of the sea surface temperatures in the equatorial central and eastern Pacific have been linked to persistent regional and global atmospheric anomalies (Shabbar and Khandekar, 1996). El Niño has been shown to have global impact on the atmospheric circulation, the most prominent of the Northern Hemisphere mid-latitude atmospheric circulation anomalies being the Pacific/North American (PNA) oscillation which affects most of North America (Wallace and Gutzler, 1981).

The NAO is the dominant source of the Northern Hemisphere climatic variability. It accounts for one-third of the total variance in the hemispheric pressure data (Rogers, 1984; Hurrell, 1995; Hurrell and van Loon, 1997). Analyzing the 1900-1983 winter NAO index, Rogers (1984) showed prominent spectral peaks at around 20 years and 7.3-8.0 years. Using a much longer winter NAO index data (1865-1994), Hurrell and van Loon (1997) identified spectral peaks at 2- to 3-year

period, 6- to 10-year period, and inter-decadal period bands. They also obtained a smooth time-frequency spectrum which showed that the 2- to 3-year period band is most prominent in the earlier part of the record, while the 6- to 10-year period band "has become more pronounced over the latter half of this century."

A thorough understanding of the temporal relationship between the NAO and ENSO is essential in elucidating the Northern Hemisphere mid-latitude climatic variability. Past studies attempted to find some association between the NAO and SO. Rogers (1984) found a large amplitude in the cospectrum between these two time series at a period of 5.7 years. Indeed, both the NAO and ENSO are characterized by fluctuations on various time scales, and changes in "Rossby-wave characteristics may at times link the NAO and the SO, but other times they may be unassociated" (Rogers, 1984). In this study, we employ a generalized wavelet transform to present evidence of the temporal structure of the spectral association between the NAO and ENSO at the 2- to 4-year and 5- to 6-year bands, documenting associated changes in the atmospheric circulation patterns.

2. Methodology

Based on the multiresolution Fourier transform (Wilson et al., 1992; Huang et al., 1997), we can define the multiresolution cross-spectral density as

$$S_{12}(f, \tau) = S_1(f, \tau)S_2^*(f, \tau) \quad (1)$$

where S_1 and S_2 are the multiresolution Fourier spectrum of the two time series $x_1(t)$ and $x_2(t)$, respectively, and * signifies complex conjugate.

In this study, we use a 131-year time series of the monthly NAO index and the Niño3 SST from January 1865 through December 1995. The NAO index used here is the one defined by Hurrell (1995), who used the difference in sea level pressure between Lisbon, Portugal and Stykkisholmur, Iceland. Because an NAO index based on station pressure is affected by small scale and transient meteorological phenomena unrelated to the NAO, the index is smoothed using a 7-point low-pass running mean filter to remove fluctuations with periods roughly less than six months. In the present study, this smoothed data constitute our NAO index data base. The Niño3 SST index, which is used as a

Copyright 1998 by the American Geophysical Union.

Paper number 98GL01936.
0094-8534/98/98GL-01936\$05.00

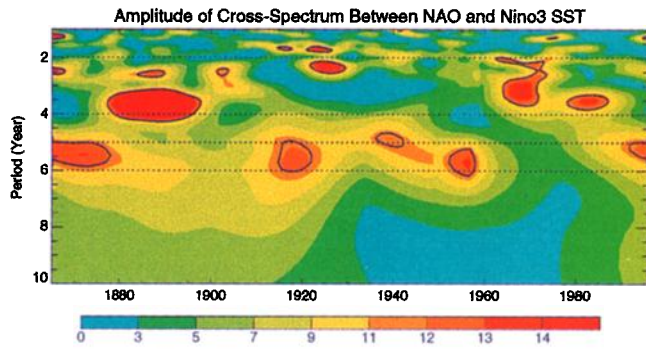


Figure 1. The amplitude of multiresolution cross-spectrum between the NAO and the Niño3 SST indices, as a function of period and time. The solid lines enclose regions of statistical significance greater than the 95% confidence level. The dashed lines indicate 2- to 4-year and 5- to 6-year period bands.

measure of the amplitude of an ENSO event, is defined as the monthly SST averaged over the eastern half of the tropical Pacific ($5^{\circ}S - 5^{\circ}N, 90^{\circ}W - 150^{\circ}W$). The index used here is the version prepared by Kaplan et al. (1998) which originally came from the U.K. Meteorological Office. The SST index is updated from 1991 to 1995 using data from NCEP, NOAA in Washington D.C..

3. Results and Discussion

Figure 1 shows the amplitude of multiresolution cross-spectrum between the time series of the NAO index and the Niño3 SST as a function of period and time. The procedure for calculating statistical significance

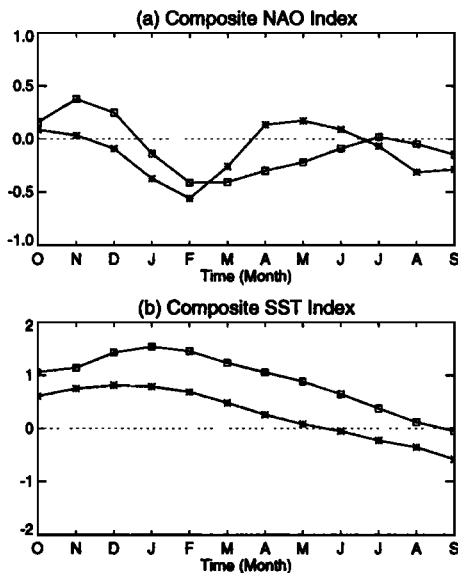


Figure 2. (a) Composite NAO index associated with the coherent year (square) and the incoherent year (asterisk). The index is shown from October of the ENSO onset year to September of the following year. (b) Same as in (a) but for Niño3 SST.

is based on comparing theoretical wavelet spectra for white and red noise with those from the Monte Carlo results (Torrence and Compo, 1998). Consistent with Rogers (1984) result of the cospectral relationship at a period of 5.7 years, Fig. 1 shows a cross-coherence be-

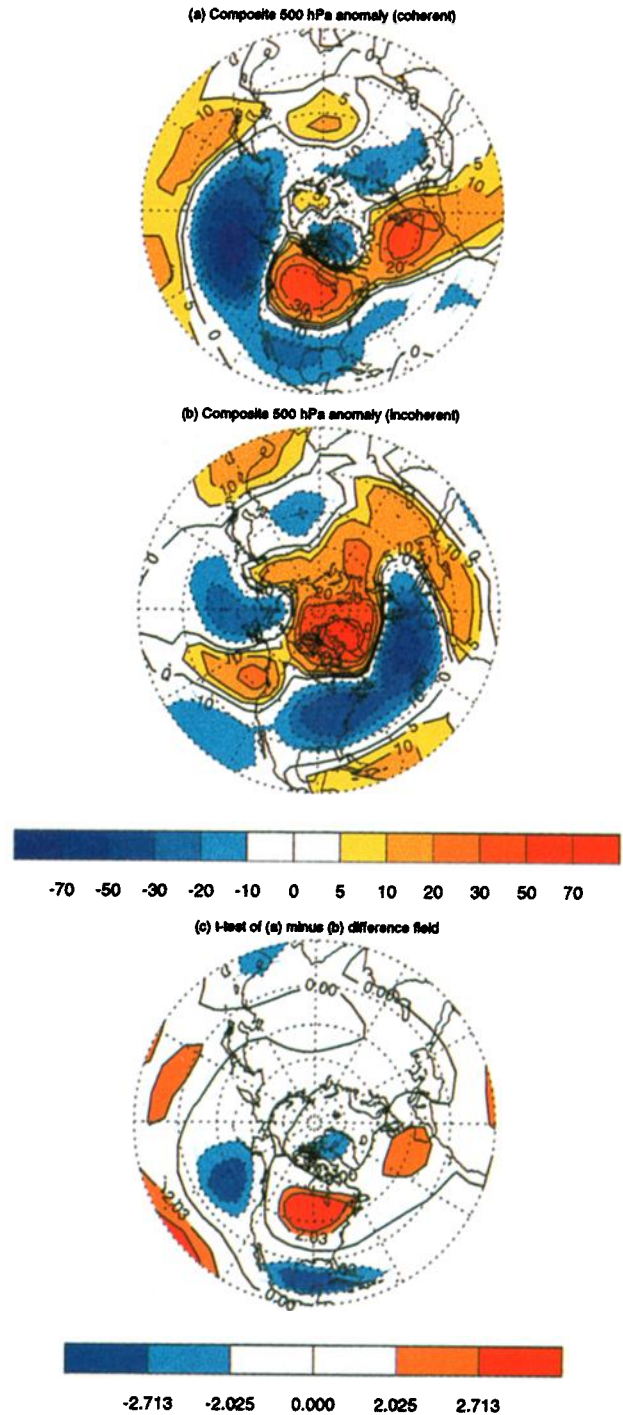


Figure 3. (a) Composite 500 hPa height anomaly field, in decameters (dams), of the winter (December through March) associated with coherent ENSO year. (b) Same as in (a) but for incoherent ENSO years. (c) t-test of the (a) minus (b) difference field. Colored areas indicate statistical significance greater than 95% confidence level.

tween the NAO index and the Niño3 SST index in a 5- to 6-year period band. It is not, however, invariant with respect to time. Statistically significant coherence at this period band is evident during the earlier part of the record, followed by a period of coherence from around 1910 to 1960 enclosing three regions of statistical significance. The association between the NAO and ENSO in this 5- to 6-year band seems to disappear almost completely from 1960 to 1990.

Another period band of the NAO-ENSO association identifiable in Fig. 1 appears to occur at periods between 2 to 4 years. The association at this 2- to 4-year period band is also not invariant with respect to time. Strong coherence is dominant in this period band during the last 20 years of the 19th century, which is consistent with the existence of a prominent 2- to 3-year periodicity during the earlier part of the NAO index as analyzed by Hurrell and van Loon (1997), as well as from 1960 to 1990. Cross-coherence between the NAO and ENSO at this period band is almost non-existent from around 1900 to 1960, a period during which cross-coherence in the 5- to 6-year period band is rather strong. The flip-flop relationship between these two period bands of the NAO-ENSO association is also evident from the beginning of the record to 1900, as well as from 1960 to 1990. Variability in the 5- to 6-year period band becomes apparent after it diminishes in the 2- to 4-year period band around 1990. All significant coherent events appear to be associated with the moderate to strong ENSO events, resulting in a distinctive pattern in the relationship between the NAO and ENSO to emerge.

The above description of the cross-coherence spectrum suggests an influence of ENSO on the NAO. Further evidence to support this comes from the results obtained by Wang and Wang (1996). In their wavelet analysis of the 124 years (1872-1995) of Darwin sea-level

pressure (a surrogate for the SO index), they found that the SO is modulated by 3- to 4-year oscillations during the first 30 to 40 years of the record. From around 1910 to 1960, the record shows oscillations in the 5- to 7-year period, with the 5- to 6-year period dominating the 1940-1960 period. The temporal characterization of the spectral structure presented by Wang and Wang (1996) is in overall structural agreement with the NAO-ENSO cross-coherence spectrum.

Listed in Table 1 are the years in which the NAO mode was coherent (E1 and E2) and incoherent (E*) with respect to the Niño3 SST index during the 27 El Niño events from 1900 to 1995. Years of El Niño events are based on Table 3.1 of Cayan and Webb (1992), which has been updated to 1995. During the 19 (9 of E1 and 10 of E2) El Niño years, which constitute about 70% of the total 27 events since 1900, the NAO and Niño3 SST indices show significant coherence at the 95% confidence level; but of the remaining 30%, or 8 El Niño years (E*), they show no coherence. Of the above 19 coherent events, the NAO index is related to the Niño3 SST index in 9 (33%) of the events at the 5- to 6-year period band (E1), and the remaining 10 events (37%) at the 2- to 4-year period band (E2).

Figure 2 shows a composite NAO and Niño3 SST indices from the onset of the El Niño year to the following year for the coherent (E1 and E2) and incoherent (E*) cases. The composite years are obtained from Table 1. For the coherent case (E1 and E2) the NAO index changes from positive to negative value from about December to January, reaching minimum in February. For the incoherent El Niño years (E*), the NAO index moves towards negative values from near zero in October and November, reaching a lower minimum than that for the coherent case in February. The negative index value persists for another four months or so for the coherent case, but only about two months for E* where the index returns to positive value by spring. Figure 2(b) shows Niño3 SST anomalies associated with coherent and incoherent years. This clearly indicates that the Niño3 SST is significantly weaker in the incoherent than in coherent years.

Changes in the Niño3 SST and NAO indices are often accompanied by changes in the atmospheric circulation patterns over the Northern Hemisphere. In order to explore the physical basis for the significant coherence between the NAO and the moderate to strong ENSO events, we compare the composite winter (DJFM, following Hurrell (1995)) 500 hPa height anomalies associated with the coherent (E1 and E2) and incoherent (E*) years as shown in Fig. 3. For the coherent case, a set of 5 years from the E1 and E2 columns in Table 1 are chosen to construct a composite 500 hPa winter anomaly field shown in Fig. 3(a), while all the 5 years since 1946 (beginning of the 500 hPa height data) from the E* column are used for the incoherent case. The overall qualitative form of the anomaly pattern shown in Fig. 3(a) for the coherent case is relatively indepen-

Table 1. The years in which the NAO mode is coherent (at the 95% confidence level) or incoherent with Niño3 SST during El Niño years since 1900. E1 refers to the years in which the NAO mode is coherent with Niño3 SST at a period of 5- to 6-year oscillation, while E2 at a period of 2- to 4-year oscillation. E* denotes the years in which the NAO and Niño3 SST are not coherent.

E1	E2	E*
1914-1915	1900-1901	1905-1906
1918-1919	1902-1903	1911-1912
1939-1940	1923-1924	1932-1933
1940-1941	1925-1926	1946-1947
1941-1942	1930-1931	1951-1952
1953-1954	1965-1966	1963-1964
1957-1958	1969-1970	1976-1977
1991-1992	1972-1973	1977-1978
1993-1994	1982-1983	
	1986-1987	
33.3%	37.1%	29.6%

dent, with few exceptions, of any 5 years out of the 9 E1 and E2 cases chosen since 1946 to construct it.

The dominant 500 hPa teleconnection pattern associated with E1 and E2, shown in Fig. 3(a), appears to be characterized by height anomaly distribution resembling a positive phase of the PNA pattern, with a positive anomaly center over the tropical North Pacific, a negative anomaly over the northern North Pacific, followed by a positive anomaly over most of Canada. A negative anomaly center is located over the southern U.S. and Mexico. Also evident is a positive anomaly center over the North Atlantic west of Europe. A pattern resembling the positive phase of the NAO can also be identified over the North Atlantic region.

For the incoherent case, associated mostly with weak ENSO events, the dominant winter 500 hPa atmospheric circulation anomaly field is shown in Fig. 3(b). Negative and positive anomalies over the western and eastern North Pacific, respectively, are present. A large zonal band of strong negative anomaly stretches from U.S. -southern Canada, across the Atlantic Ocean to western Europe, and is bordered to the north by an area of predominantly positive anomaly located over northern Canada and Greenland. This negative phase of the NAO is consistent with the result shown in Fig. 2(a).

Figure 3(c) shows regions of statistical significance (using the t-test with sample size of 20 points for each grid) for a difference field constructed by subtracting Fig. 3(b) from Fig. 3(a). The significance pattern shows that in the coherent winter case, an enhanced positive phase of PNA pattern is likely to occur with the positive phase of the NAO. This explains why the NAO and the Niño3 SST are generally incoherent during E* events, when the tropical Pacific SST anomalies are generally weak during E* events to force any particular distinctive teleconnection pattern to act as a viable linkage or "bridge" between the NAO and tropical SST anomalies. Figure 3(c) is also indicative of the fact that the anomaly pattern shown in Fig. 3(a) is less variable (i.e., more stable) than the pattern shown in Fig. 3(b).

The coherent relationship between the NAO and the Niño3 SST indices indicates that the ENSO modulates the NAO variation through wavelike patterns (such as the PNA) which would change the jet stream and storm track locations over the North Atlantic. Typically, a strong ENSO event initiates a northward Rossby wave propagation from the tropical Pacific to northern North America. This is reflected in the generation of a dominant standing wave train pattern resembling PNA

(Hoskins and Karoly, 1981). It is, therefore, our conjecture that during a weak ENSO event, a clear signature of the PNA pattern is absent, preventing any "influential" energy propagation toward the North Atlantic.

Acknowledgments. We would like to thank the two reviewers for their insightful comments and suggestions.

References

- Cayan, D.R. and R.H. Webb, El Niño/Southern Oscillation and streamflow in the western United States, in *El Niño: Historical and Paleoclimatic Aspects of the Southern Oscillation*, edited by Diaz, H.F. and Markgraf, V., pp. 29-68, Cambridge University Press, 1992.
- Hoskins, B. J. and D. Karoly, The steady linear response of a spherical atmosphere to thermal and orographic forcing, *J. Atmos. Sci.*, **38**, 1179-1196, 1981.
- Huang, J.-P., K. Higuchi and N.B.A. Trivett, Multiresolution Fourier transform and its application on analysis of CO₂ fluctuations over Alert, *J. Meteor. Soc. Japan*, **75**, 701-715, 1997.
- Hurrell, J.W., Decadal trends in the North Atlantic Oscillation: regional temperatures and precipitation, *Science*, **269**, 676-679, 1995.
- Hurrell, J.W. and H. van Loon, Decadal variations in climate associated with the North Atlantic Oscillation, *Climate Change*, **36**, 301-326, 1997.
- Kaplan, A., M. Cane, Y. Kushnir, A.C. Clement, M.B. Blumenthal and B. Rajagopalan, Analyses of global sea surface temperature 1856-1991, *J. Geophys. Res.*, in press, 1998.
- Rogers, J.C., The association between the North Atlantic Oscillation and the Southern Oscillation in the Northern Hemisphere, *Mon. Wea. Rev.*, **112**, 1999-2015, 1984.
- Shabbar, A. and M. Khandekar, The impact of El Niño-Southern Oscillation on the temperature field over Canada, *Atmosphere-Ocean*, **34**, 401-416, 1996.
- Torrence, C. and G.P. Compo, A practical guide to wavelet analysis, *Bull. Am. Meteor. Soc.*, **79**, 61-78, 1998.
- Wang, B. and Y. Wang, Temporal structure of the Southern Oscillation as revealed by waveform and wavelet analysis, *J. Climate*, **9**, 1586-1598, 1996.
- Wallace, J.M. and D.S. Gutzler, Teleconnections in the geopotential height field during the Northern Hemisphere winter, *Mon. Wea. Rev.*, **109**, 784-812, 1981.
- Wilson, R., A.D. Calway and E.R.S. Pearson, A generalized wavelet transform for Fourier analysis: the multiresolution Fourier transform and its application to image and audio signal analysis, *Info. Theory*, **38**, 674-690, 1992.

Jianping Huang, Kaz Higuchi and Amir Shabbar
Atmospheric Environment Service, Environment Canada
4905 Dufferin Street, Downsview, Ontario, M3H 5T4,
Canada e-mail: Jianping.Huang@ec.gc.ca

(Received February 17, 1998; revised April 23, 1998;
accepted May 27, 1998.)